



Short communication

Beneficial effects of 1-propylphosphonic acid cyclic anhydride as an electrolyte additive on the electrochemical properties of $\text{LiNi}_{0.5}\text{Mn}_{1.5}\text{O}_4$ cathode material



Guochun Yan, Xinhai Li*, Zhixing Wang, Huajun Guo, Xunhui Xiong

School of Metallurgy and Environment, Central South University, Changsha 410083, PR China

HIGHLIGHTS

- 1-Propylphosphonic acid cyclic anhydride (PACA) is investigated as an additive.
- Self-discharge of $\text{LiNi}_{0.5}\text{Mn}_{1.5}\text{O}_4$ is effectively suppressed by adding PACA into electrolyte.
- Enhanced cycling performance of $\text{LiNi}_{0.5}\text{Mn}_{1.5}\text{O}_4$ at elevated temperatures is achieved.
- Reduced transition metal dissolution of $\text{LiNi}_{0.5}\text{Mn}_{1.5}\text{O}_4$ by using PACA.

ARTICLE INFO

Article history:

Received 21 February 2014

Received in revised form

8 April 2014

Accepted 13 April 2014

Available online 25 April 2014

Keywords:

1-Propylphosphonic acid cyclic anhydride

Additive

Spinel lithium–nickel–manganese oxide

Electrochemical properties

ABSTRACT

Self-discharge and transition metal dissolution weaknesses bother the application of $\text{LiNi}_{0.5}\text{Mn}_{1.5}\text{O}_4$ cathode material due to the severe oxidation of electrolyte at the high voltage state. A novel additive, 1-propylphosphonic acid cyclic anhydride (PACA), is desirable to prevent this oxidation. CV and charge–discharge results reveal that adding 0.5% PACA can relieve the oxidation of electrolyte. Consequently, the self-discharge and transition metal dissolution are both suppressed effectively, which is validated by self-discharge tests, XPS, and EDX analyses. Moreover, using PACA as an additive enhances the capacity retention capability of $\text{LiNi}_{0.5}\text{Mn}_{1.5}\text{O}_4$ at elevated temperatures significantly.

Crown Copyright © 2014 Published by Elsevier B.V. All rights reserved.

1. Introduction

Lithium ion batteries (LIBs) are widely used as power sources for a variety of devices, such as consumer electronics, electric tools, and electric vehicles [1,2]. The development of LIBs requires higher energy density, and using high operating voltage (>4.5 V vs. Li/Li^+) cathode materials is a commonly accepted method. During the past few decades, cathode materials with a high discharge voltage have been proposed, for example, olivine-type LiNiPO_4 [3], and LiCoPO_4 [4], spinel-type $\text{LiNi}_{0.5}\text{Mn}_{1.5}\text{O}_4$ [5] and LiCoMnO_4 [6]. Among these alternatives, $\text{LiNi}_{0.5}\text{Mn}_{1.5}\text{O}_4$ is the most attractive and promising material because of the moderate theoretical specific capacity (147 mAh g^{-1}) and relatively high operating voltage plateau at around 4.7 V [7]. However, several issues, including oxidation of the

electrolyte at high voltage, severe self-discharge, and transition metal dissolution, should be addressed before its implementation [8–11].

The problems mentioned above are mainly caused by the parasitic reactions at the interface between the cathode material and the electrolyte. It is well known that the trace of water in the electrolyte will generate HF in LiPF_6 -based electrolyte, facilitating the decomposition of electrolyte, eroding the surface of cathode material, and deteriorating the electrochemical performance of cathode material [9,12]. In addition, the main solvent of electrolyte, like ethylene carbonate, decomposes severely under high voltage state. Therefore, to enhance the electrochemical performance of $\text{LiNi}_{0.5}\text{Mn}_{1.5}\text{O}_4$, keeping the stability of electrolyte is a vital factor. On the one hand, surface coating was demonstrated an effective way to prevent the side reaction in the cathode/electrolyte interface. On the other hand, exploring solvents supporting high operating voltage, such as fluorinated esters and ethers [13,14], ionic liquids [15,16], and sulfones [17–19], is also considered a useful and

* Corresponding author. Tel./fax: +86 731 88836633.

E-mail address: xinhai-li@csu.edu.cn (X. Li).

practical method to resolve the instability of electrolyte under high voltage. In addition, many film-forming additives, for instance, glutaric anhydride (GA) [20], succinic anhydride (SA) [21], and lithium bis(oxalato)borate (LiBOB) [22], can form a stable film at the surface of $\text{LiNi}_{0.5}\text{Mn}_{1.5}\text{O}_4$ cathode material. Previous studies have confirmed that the strategy is beneficial to enhance the cycling capability at room and elevated temperatures and suppress the self-discharge and transition metal dissolution [20–23].

The key idea of these film-forming additives for high voltage is to form a stable film at the surface of cathode material, segregating the interaction between the cathode material and the electrolyte. Generally, the additive will decompose prior to the main solvent of the electrolyte, then the decomposition products cover the active sites of the cathode material, avoiding the catalytic action of the transition metal ions at high voltage state (like Ni^{4+}). Thus, we should look for an additive with lower oxidation potential, or the possibility to be polymerized during the charge process. Furthermore, a large volume of literature suggests that phosphate-based compounds and anhydrides are promising candidates for high voltage additives [20,21,24–26]. In addition, a phosphate compound, tris(trimethylsilyl)phosphate, was introduced successfully as a film-forming additive for the high voltage electrolyte in our previous study. PACA is a powerful coupling reagent and water scavenger in organic synthesis [27,28]. Hence, PACA may remove the trace water in the electrolyte. In addition, the intermediate products from the dehydration reaction may polymerize at the cathode surface to improve the interface between the cathode and the electrolyte.

Bearing this in mind, we investigated a cyclic anhydride, PACA, as a novel additive for high voltage electrolyte using Li/ $\text{LiNi}_{0.5}\text{Mn}_{1.5}\text{O}_4$ half-cells in this study. It has not been reported before as an electrolyte additive for $\text{LiNi}_{0.5}\text{Mn}_{1.5}\text{O}_4$ cathode material as far as we know. Moreover, we expect that it will polymerize to form a stable protecting layer at the cathode surface, enhancing the electrochemical performance of $\text{LiNi}_{0.5}\text{Mn}_{1.5}\text{O}_4$.

2. Experimental

2.1. Electrode preparation

The electrolyte consisting of ethylene carbonate (EC)/ethyl methyl carbonate (EMC) (3:7 in wt. ratio) containing 1 M (1 M = 1 mol L⁻¹) LiPF_6 (marked as BE) was kindly provided by the Jiangxi Youli New Materials Co. Ltd. The PACA solution (50 wt. % in ethyl acetate) was purchased from Protech Science Corp. (USA), and it was added to BE to a final PACA wt. % of 0.5% without further purification in the glove box under Ar atmosphere. The $\text{LiNi}_{0.5}\text{Mn}_{1.5}\text{O}_4$ (Xing Neng New Materials Co. Ltd, China) electrode was prepared by mixing 80 wt. % cathode materials, 10 wt. % Super P carbon, 10 wt. % polyvinylidene fluoride (PVDF), coating on an aluminum foil.

2.2. Electrochemical tests

Cyclic voltammetry experiments were performed with an Electrochemical Workstation (CHI604E, Chenhua, China) at a sweep rate of 0.1 mV s⁻¹. The electrochemical impedance spectra (EIS) of the cells at 100% state of charge (SOC) after 25 and 50 cycles were measured over a frequency range from 100 kHz to 0.01 Hz. Self-discharge tests were performed according to the following procedure. First, the fresh cells were charged to a cut-off voltage to 4.9 V with a constant current of 0.2 C ($1\text{C} = 110 \text{ mA g}^{-1}$), followed by a constant voltage charge to a cut-off current to 0.05 C. Then, the cells were left under OCV conditions for 336 h (2 weeks). Electrochemical charge–discharge tests were performed with 2025 coin-

type cells utilizing a Neware battery cycler between 3.5 and 4.9 V (vs. Li/Li^+) at room temperature.

2.3. Ex situ characterization of the cycled $\text{LiNi}_{0.5}\text{Mn}_{1.5}\text{O}_4$ and the separator

To analyze the surface composition of the cycled electrode, the cells were disassembled in the glove box filled with Ar gas. The cathode was washed by high purity dimethyl carbonate (DMC) three times to remove the electrolyte residue under magnetic stirring, and then was dried in vacuum box at 40 °C for 6 h. For the purpose to detect the transition metal dissolution, the separator was not washed by DMC. The crystal structure of the cathode electrodes were determined by X-ray diffraction (XRD, Cu K α radiation, Rint-2000, Rigaku). The morphology of the cathode electrodes and separator were observed by a scanning electron microscope (SEM, Sirion 200). The elements at the surface of the separator were identified by energy dispersive X-ray spectroscopy (EDX). X-ray photoelectron spectroscopy (XPS, PHI 5600, Perkin–Elmer) was employed to identify the element composition at the cathode surface. Fourier transform infrared (FTIR) spectra of the electrode were recorded by a Nicolet AVATAR 360 FT-IR spectrometer.

3. Results and discussion

Fig. 1(a) shows the charge–discharge curves of Li/ $\text{LiNi}_{0.5}\text{Mn}_{1.5}\text{O}_4$ cells at 0.2 C in the electrolyte with and without PACA. As expected,

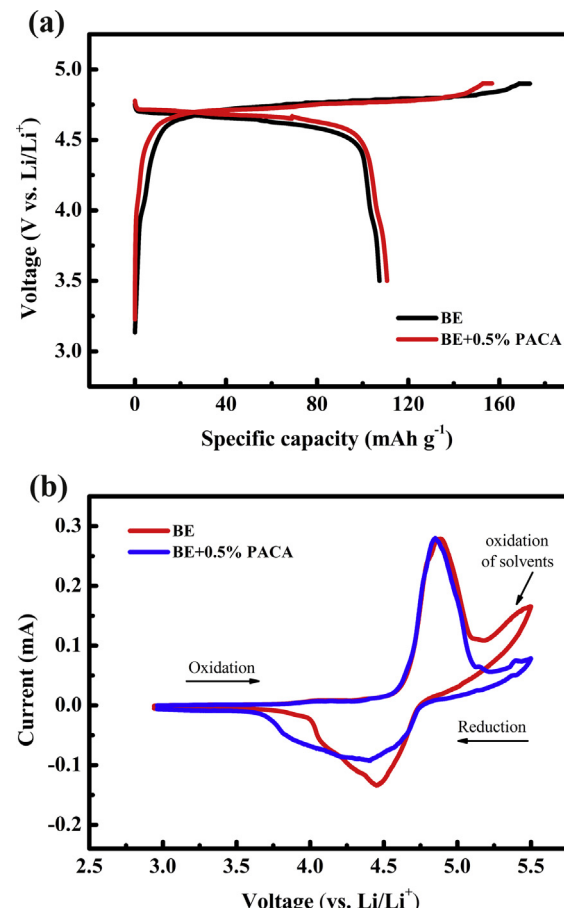


Fig. 1. The charge–discharge curves (a), and the cyclic voltammograms (b) of the $\text{Li}/\text{LiNi}_{0.5}\text{Mn}_{1.5}\text{O}_4$ cells in the electrolyte with and without PACA.

the charge capacity (156.8 mAh g^{-1}) of the cell with PACA is decreased compared with that without PACA (173.5 mAh g^{-1}), indicating that the solid electrolyte interface with the participating of PACA can prevent the severe decomposition of the solvent. Therefore, the initial coulombic efficiency (70.60%) of the cell with PACA is higher than that without PACA (61.90%). In addition, we can see that there is a strong oxidation peak at around 5.2 V in the cells without PACA from Fig. 1(b), while it does not appear in the cells with 0.5% PACA. The result is consistent with the charge–discharge curves, demonstrating that the addition of PACA can decrease the solvent decomposition effectively. Moreover, the anodic peak (about 4.85 V) is corresponding to the oxidation of the Ni^{2+} , and the cathodic peak around 4.45 V can be attributed to the reduction of Ni^{4+} . The redox voltage difference is as high as 0.40 V, which implies the polarization of the $\text{LiNi}_{0.5}\text{Mn}_{1.5}\text{O}_4$ cathode material used in our study is severe. It is the main reason why the coulombic efficiencies of the cells with and without PACA are both lower than that represented in other literature [24,29].

As shown in Fig. 2(a), the cycling performance of the cell cycled in BE sample is almost the same with that the cell cycled in BE + 0.5% PACA sample. The discharge capacity of the $\text{LiNi}_{0.5}\text{Mn}_{1.5}\text{O}_4$ cycled in the electrolyte with PACA is just slightly higher than that without PACA. It should be noted that the discharge capacity at 25 cycles is decreased apparently, especially for the cell cycled in the electrolyte without PACA. In our test procedure, the cell waits for the EIS test after 25 cycles at 100% SOC, and the following discharge test is declared a couple of hours. This phenomenon reminds us that there exists a severe self-discharge of the $\text{LiNi}_{0.5}\text{Mn}_{1.5}\text{O}_4$ cathode material, which was confirmed by the previous study [9,21]. In addition, we tracked the coulombic efficiency of the cells during the cycling process at a relatively low C rate (0.2 C) because it can reflect the situation of electrolyte oxidation [9]. It can be seen apparently that the coulombic efficiency of the cells with PACA is improved in comparison with the cells without PACA from Fig. 2(b).

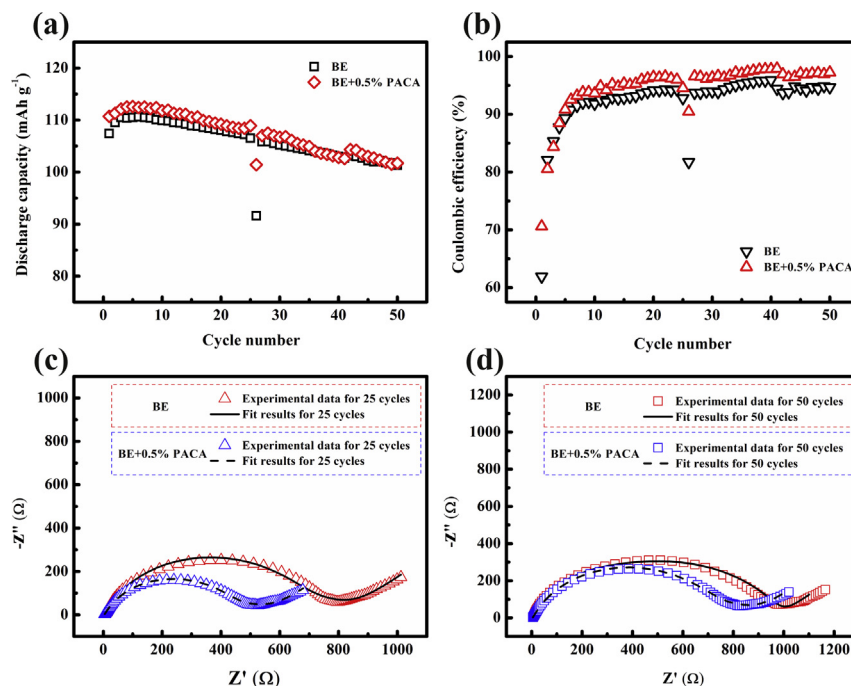


Fig. 2. The cycling performance (a), and the coulombic efficiency (b) of the $\text{Li}/\text{LiNi}_{0.5}\text{Mn}_{1.5}\text{O}_4$ cells with and without PACA; the EIS of the $\text{Li}/\text{LiNi}_{0.5}\text{Mn}_{1.5}\text{O}_4$ cells with and without PACA after 25 cycles (c), 50 cycles (d).

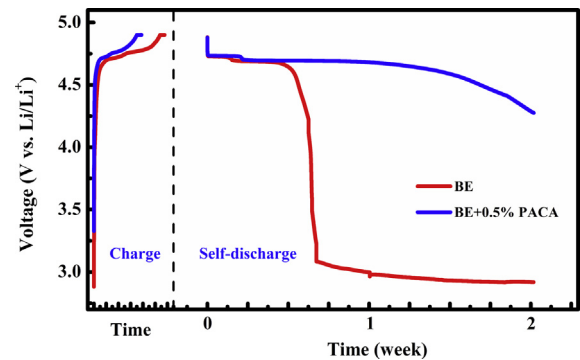


Fig. 3. The OCV– t curves of the $\text{Li}/\text{LiNi}_{0.5}\text{Mn}_{1.5}\text{O}_4$ cells in the electrolyte with and without PACA after having been fully charged (100% SOC) for 336 h.

Generally, the PF_5 (comes from the lithium salt, LiPF_6) will react with the trace water of the electrolyte to generate HF. Meanwhile, the decomposition products of carbonate solvents (Li_2CO_3 , ROLi) will interact with HF to generate LiF, which will deposit at the surface of the cathode material. Thus, the more decomposition of the carbonate solvents proceeds, the more LiF is in the solid electrolyte interface. In addition, more content of the LiF at the surface will increase the impedance of the cell due to the poor electrical conductivity. EIS results of the cells after 25 and 50 cycles reveal that impedance of the cells with PACA is reduced as can be seen in Fig. 2(c) and (d). The results of charge–discharge and EIS tests demonstrate that the addition of PACA is beneficial to suppress the decomposition of electrolyte through stabilizing the solid electrolyte interface at the cathode surface.

To verify the discharge capacity-dropping phenomenon mentioned above, the self-discharge tests were carried out and the results are presented in Fig. 3. Interestingly, the OCV– t curves are very familiar with the discharge curves of the $\text{LiNi}_{0.5}\text{Mn}_{1.5}\text{O}_4$

cathode material. There are two plateaus in the OCV– t curves for both cells in the electrolyte with and without PACA. During the self-discharge process, the fully charged state $\text{LiNi}_{0.5}\text{Mn}_{1.5}\text{O}_4$ ($\text{Ni}_{0.5}\text{Mn}_{1.5}\text{O}_4$) will catalyze oxidation of electrolyte, and the Ni^{4+} will be reduced to form $\text{Li}_x\text{Ni}_{0.5}\text{Mn}_{1.5}\text{O}_4$. The one around 4.74 V is ascribed to the reduction of Ni^{4+} to Ni^{3+} , and the other located around 4.7 V is assigned to the reduction of Ni^{3+} to Ni^{2+} . The two plateaus at about 4.7 V associate with the lithium ions insertion into 8a tetrahedral sites of the cubic spinel structure. In addition, the prolonged plateau around 2.90 V in the OCV– t curve of the BE sample is attributed to the reduction of Mn^{4+} to Mn^{3+} involving Li^+ ions insertion into 16c octahedral sites of the spinel structure [11]. Furthermore, the OCV of the cells with 0.5% PACA can maintain 4.27 V after 336 h (2 weeks). In contrast, the OCV of the cells with BE sample drops to 2.90 V after 336 h. The results are in accordance with the analyses of the charge–discharge experimental data, namely the self-discharge is suppressed considerably when the additive is introduced into the electrolyte.

Infrared spectroscopy has been confirmed a useful tool to identify the cation ordering in $\text{LiNi}_{0.5}\text{Mn}_{1.5}\text{O}_4$ [11,15,30,31]. In order to figure out the reason that the addition of PACA restrains the self-discharge of $\text{LiNi}_{0.5}\text{Mn}_{1.5}\text{O}_4$ cathode material, FTIR spectra of fresh $\text{LiNi}_{0.5}\text{Mn}_{1.5}\text{O}_4$ and cycled $\text{LiNi}_{0.5}\text{Mn}_{1.5}\text{O}_4$ electrode samples were obtained as shown in Fig. 4(a). As we can see clearly, two IR modes around 500 and 621 cm^{-1} are both split into several components in all three samples, which illustrate that the fresh and cycled samples are ordered spinel structure because the IR modes at 500 and

621 cm^{-1} will not be split in a disordered spinel structure [11,29]. Moreover, we obtained the XRD patterns of the fresh $\text{LiNi}_{0.5}\text{Mn}_{1.5}\text{O}_4$ and cycled $\text{LiNi}_{0.5}\text{Mn}_{1.5}\text{O}_4$ electrode as shown in Fig. 4(b). All Bragg peaks in $\text{LiNi}_{0.5}\text{Mn}_{1.5}\text{O}_4$ electrode samples are matched well with the reference peak positions of $\text{LiNi}_{0.5}\text{Mn}_{1.5}\text{O}_4$ (JCPDS# 80-2126) except the peaks ascribed to the Al current collector. The results are in good agreement with the IR analyses. Therefore, the spinel structure is not destroyed based on the IR and XRD analyses even though the $\text{LiNi}_{0.5}\text{Mn}_{1.5}\text{O}_4$ electrode displays a severe self-discharge. It also can be proved by the excellent cyclic capability of the $\text{LiNi}_{0.5}\text{Mn}_{1.5}\text{O}_4$ as shown in Fig. 2(a).

Fig. 5 shows the SEM images of fresh $\text{LiNi}_{0.5}\text{Mn}_{1.5}\text{O}_4$ (a), cycled $\text{LiNi}_{0.5}\text{Mn}_{1.5}\text{O}_4$ in the electrolyte sample BE (b) and BE + 0.5% PACA (c). The fresh $\text{LiNi}_{0.5}\text{Mn}_{1.5}\text{O}_4$ particles present a smooth surface, while the cycled $\text{LiNi}_{0.5}\text{Mn}_{1.5}\text{O}_4$ particles display a rough surface. It suggests that the decomposition products of electrolyte deposit at the surface of cathode material. In addition, it is more obvious for cycled $\text{LiNi}_{0.5}\text{Mn}_{1.5}\text{O}_4$ in the electrolyte sample BE compared with that in the electrolyte sample BE + 0.5% PACA, which indicates that the electrolyte oxidation may proceed more serious for the electrolyte sample BE.

XPS analyses are considered a valid tool to determine the valence of the element. Due to the self-discharge, the voltage of the cell is decreased obviously, and the oxidation of the electrolyte will result in the variation of the valence state of transition metal ions in $\text{Li}_x\text{Ni}_{0.5}\text{Mn}_{1.5}\text{O}_4$. It is meaningful to analyze the valence state of Ni and Mn. Fig. 6 presents the Ni 2p and Mn 2p XPS patterns of the $\text{Li}_x\text{Ni}_{0.5}\text{Mn}_{1.5}\text{O}_4$ electrode in BE and BE + 0.5% PACA sample. From Fig. 6(a) and (c), the XPS spectra of Ni 2p3/2 display a peak at 854.2 eV and a satellite peak at 860.68 eV, which are close to that reported for NiO [32,33]. In addition, the peak at 857.78 eV can be assigned to NiF_2 [10,29], which is the product of the electrolyte oxidation at the cathode surface. Thus, almost all of the Ni^{4+} at the surface of $\text{Ni}_{0.5}\text{Mn}_{1.5}\text{O}_4$ electrode with BE sample are reduced to Ni^{2+} . While for the $\text{Li}_x\text{Ni}_{0.5}\text{Mn}_{1.5}\text{O}_4$ electrode with BE + 0.5% PACA, there is a strong peak at 856.28 eV attributed to Ni^{3+} [34], except for the peaks at 854.48 and 860.98 eV ascribed to Ni^{2+} . The Mn spectrum displays two peaks because of the Mn 2p3/2 and the Mn 2p1/2 as shown in Fig. 6(b) and (d). For the $\text{Li}_x\text{Ni}_{0.5}\text{Mn}_{1.5}\text{O}_4$ electrode with BE + 0.5% PACA sample, these peaks locate in 642.18/653.98 eV, while they are slightly shifted to 641.67/653.28 eV for the $\text{Li}_x\text{Ni}_{0.5}\text{Mn}_{1.5}\text{O}_4$ electrode with BE sample. It has been found the binding energy for Mn^{4+} is higher than that for Mn^{3+} : 642.2–642.8 eV for Mn^{4+} and 641.7–642.2 eV for Mn^{3+} [35]. Therefore, there is Mn^{3+} in the $\text{Li}_x\text{Ni}_{0.5}\text{Mn}_{1.5}\text{O}_4$ with the BE sample as the peak at 641.67 eV is close to the peak for Mn^{3+} (641.7 eV). These valence variations of transition metal are in good agreement with the OCV– t curve analyses.

To investigate the effect of the PACA on the surface modification of $\text{LiNi}_{0.5}\text{Mn}_{1.5}\text{O}_4$ electrode further, XPS was employed to determine the surface composition of the fresh and cycled electrode as shown in Fig. 7, and the elements concentration was listed in Table 1. After rest for 2 weeks (it was 100% SOC before), the surface constitution varied considerably. The content of F and P at the surface of the cycled electrode is both increased compared with the fresh electrode. From Fig. 7, we can distinguish that the intensity of the peaks (678.2 eV) assigned to PVDF is the same, while the content of LiF is increased obviously. Specifically, the amount of LiF at the surface of the cycled electrode in BE + 0.5% sample (30.49%) is lesser than that in BE sample (36.31%). As for O 1s, the relative atomic ratio of Metal–O bonds in the BE sample (16.60%) is the lowest. In contrast, the amount of C=O bonds is the largest (57.90%). In addition, the intensity of P 2p for the electrode with BE sample is also stronger than that with BE + 0.5% PACA sample. These results elucidate that the decomposition of the BE

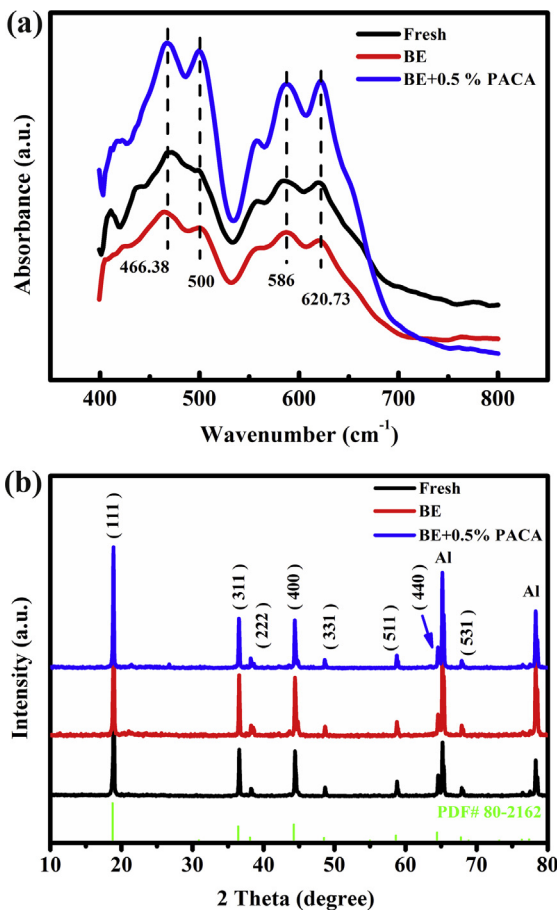


Fig. 4. The infrared spectra (a) and the XRD patterns (b) of the fresh and cycled $\text{LiNi}_{0.5}\text{Mn}_{1.5}\text{O}_4$ electrode samples.

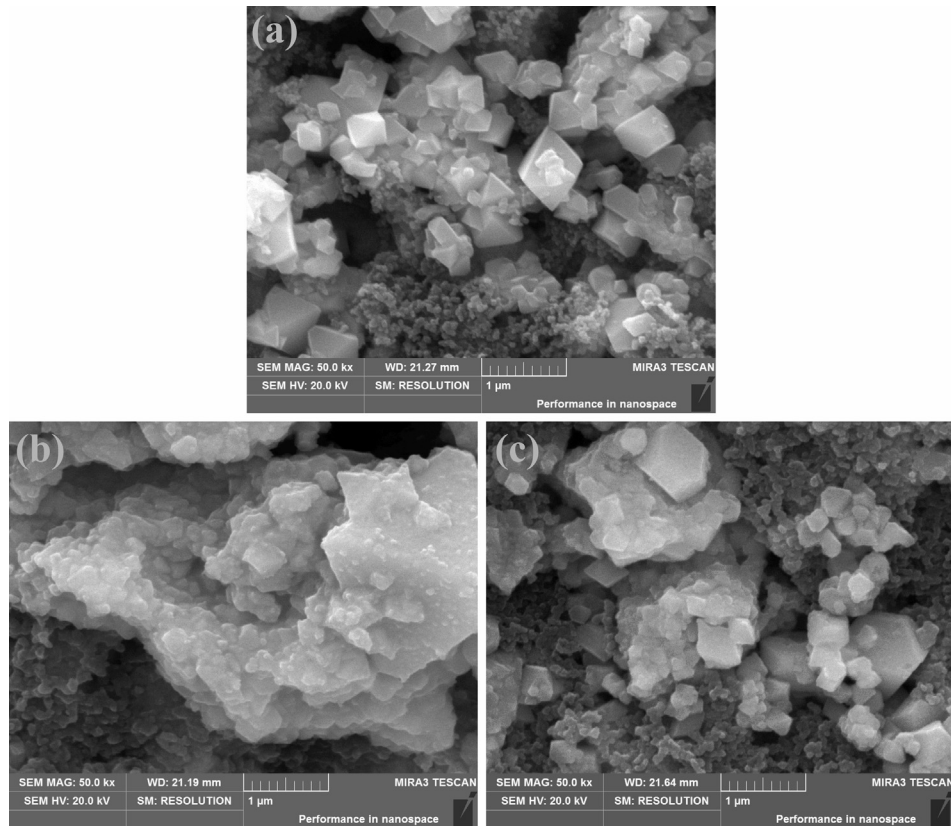


Fig. 5. The SEM images of fresh $\text{LiNi}_{0.5}\text{Mn}_{1.5}\text{O}_4$ (a), cycled $\text{LiNi}_{0.5}\text{Mn}_{1.5}\text{O}_4$ in the electrolyte sample BE (b) and BE + 0.5% PACA (c).

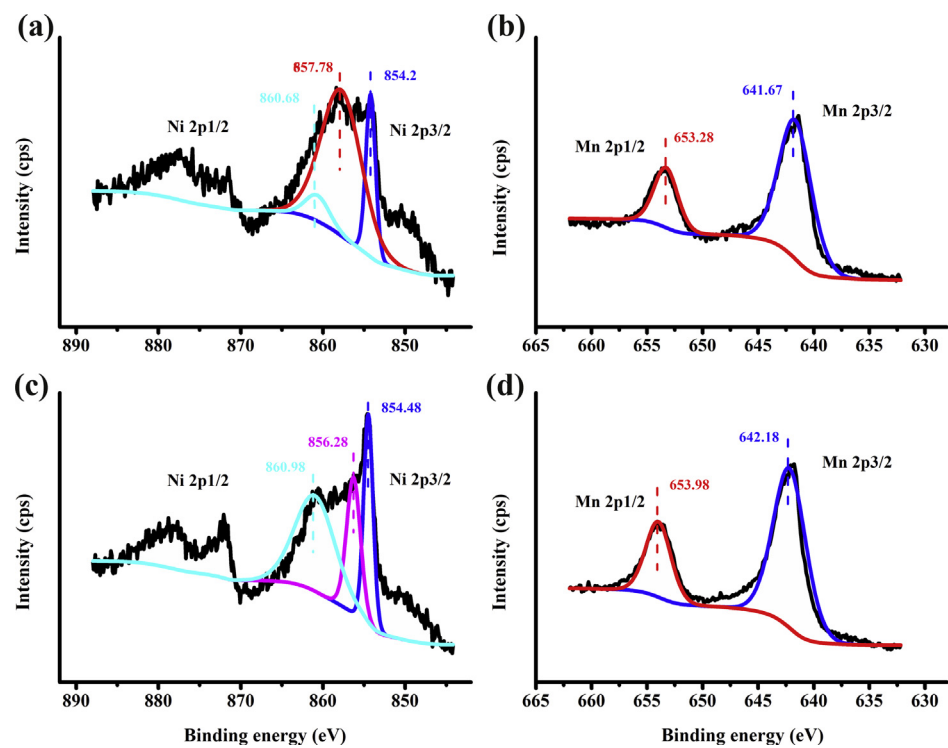


Fig. 6. The Ni 2p XPS patterns of the cycled $\text{LiNi}_{0.5}\text{Mn}_{1.5}\text{O}_4$ electrode in BE (a), and BE + 0.5% PACA (c); the Mn 2p XPS patterns of the cycled $\text{LiNi}_{0.5}\text{Mn}_{1.5}\text{O}_4$ electrode in BE (b), and BE + 0.5% PACA (d).

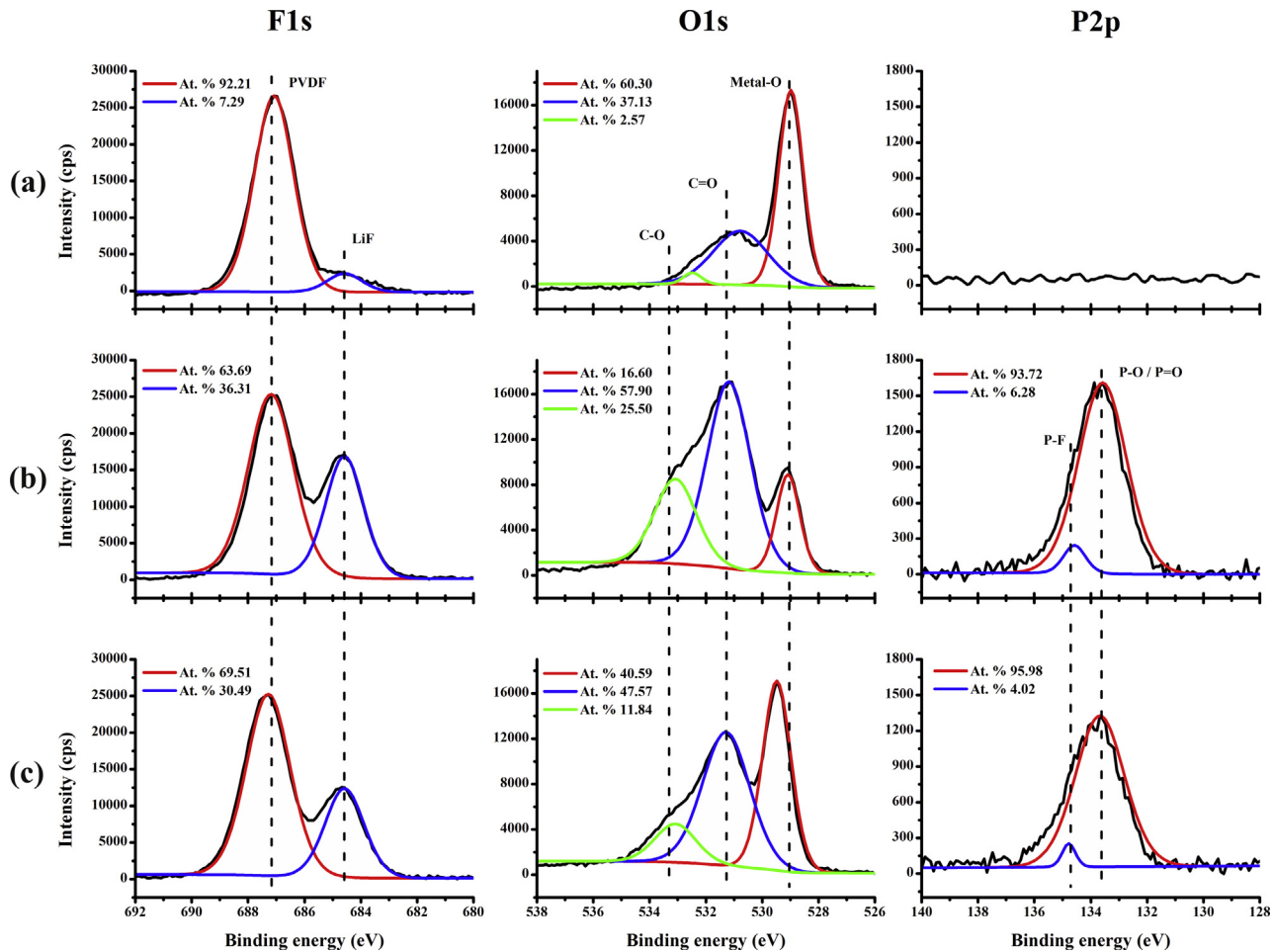


Fig. 7. The F 1s, O 1s, and P 2p XPS patterns of the fresh $\text{LiNi}_{0.5}\text{Mn}_{1.5}\text{O}_4$ electrode (a), and cycled $\text{LiNi}_{0.5}\text{Mn}_{1.5}\text{O}_4$ electrode in the electrolyte sample BE (b) and BE + 0.5% PACA (c).

electrolyte is more severe than the BE + 0.5% PACA sample. Consequently, there are more decomposition products of the electrolyte (like LiF, Li_2CO_3 , ROLI) covered at the surface of $\text{LiNi}_{0.5}\text{Mn}_{1.5}\text{O}_4$ electrode.

In consideration of the transition metal dissolution of $\text{LiNi}_{0.5}\text{Mn}_{1.5}\text{O}_4$, the EDX spectra of the fresh separator, and the cycled separator with BE and BE + 0.5% PACA samples were obtained as shown in Fig. 8. The fresh separator displays some tunnels along a specific direction, and the EDX results validate it consists of C (H cannot be detected in EDX measurement) as can be seen in Fig. 8(a). While for the separator cycled in BE electrolyte (Fig. 8(b)), it is covered with lots of deposits with a rough surface. It should be noted that the bright spot in Fig. 8(b) might be the $\text{LiNi}_{0.5}\text{Mn}_{1.5}\text{O}_4$ cathode material stuck in the separator as the Ni/Mn atomic ratio (0.3822 from the EDX result) is close to the XPS results (0.3892) from Table 1. Nevertheless, the gray area in the separator still has some Ni and Mn in it. Hence, EDX results in

different area (red rectangle) reveal that the deposits contain Ni and Mn element, which originates from the $\text{LiNi}_{0.5}\text{Mn}_{1.5}\text{O}_4$ cathode material due to the transition metal dissolution. In contrast, the separator from BE + 0.5% PACA sample shows a relatively smooth surface, and it does not contain any Ni and Mn at the surface. Based on XPS and EDX analyses, the additive can stop the transition metal dissolution of $\text{LiNi}_{0.5}\text{Mn}_{1.5}\text{O}_4$ by altering the solid surface interface.

On the basis of the self-discharge tests, SEM, XPS and EDX analyses, we proposed the mechanism of PACA as an additive to improve the electrochemical performance of $\text{LiNi}_{0.5}\text{Mn}_{1.5}\text{O}_4$ as shown in Fig. 9(a). The carbonate solvent will be oxidized at the cathode surface due to the inherent chemical instability when the charge voltage is larger than 4.5 V (vs. Li/Li^+). It will cause the transmission of electron from electrolyte to the cathode material, leading to the decrease of coulombic efficiency [21,36–38]. The oxidation of electrolyte will result in a drop of open circuit voltage (self-discharge) while the cell rest at a charged state. During the cycling performance, this severe oxidation of electrolyte may cause the transition metal dissolution, especially for the disproportionated reaction of Mn^{3+} . When the PACA is introduced into the blank electrolyte, it will polymerize at the surface of the cathode electrode, forming a stable cathode/electrolyte interface because of the P–O–M ($M = \text{Ni}, \text{Mn}$) bonds. Meanwhile, this improved solid electrolyte interface film can relieve the oxidation of carbonate solvent, enhancing the electrochemical performance of the

Table 1
The element concentration of the fresh and cycled $\text{LiNi}_{0.5}\text{Mn}_{1.5}\text{O}_4$ electrode.

Elements	Li	C	O	F	P	Ni	Mn
Fresh	2.16	64.64	13.20	16.73	/	0.84	2.43
BE	9.54	45.07	20.19	19.94	2.70	0.72	1.85
BE + 0.5% PACA	7.02	48.29	18.72	19.80	2.49	1.01	2.67

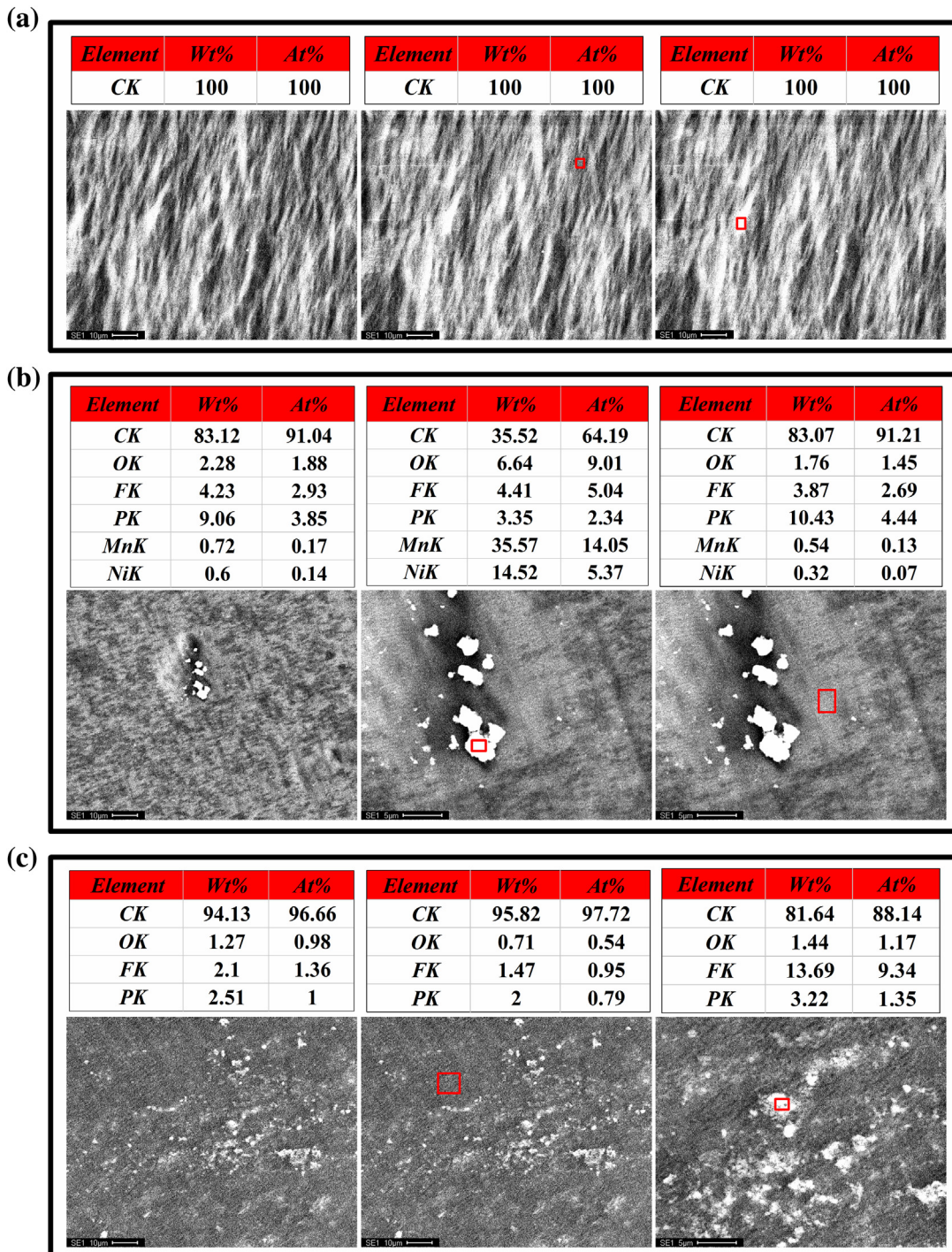


Fig. 8. The SEM images and EDX of the fresh separator (a), cycled separator in BE (b) and BE + 0.5% PACA (c) sample.

$\text{LiNi}_{0.5}\text{Mn}_{1.5}\text{O}_4$ cathode material. Moreover, the elevated temperatures will accelerate the decomposition of the carbonate solvent at high voltage state, which will deteriorate the cathode/electrolyte interface. In contrast, this parasitic reaction will be relieved with the relatively stable surface film derived from PACA. Thus, we carried out the electrochemical tests at 55 °C further, and the results are shown in Fig. 9(b). Apparently, the $\text{LiNi}_{0.5}\text{Mn}_{1.5}\text{O}_4$ electrode displays improved cycling performance at elevated temperatures when PACA is introduced to the blank electrolyte.

4. Conclusions

A cyclic anhydride additive, PACA, was successfully introduced to the electrolyte for improving the electrochemical performance of the $\text{LiNi}_{0.5}\text{Mn}_{1.5}\text{O}_4$. CV and charge–discharge tests confirmed that the electrolyte oxidation was relieved by adding 0.5% PACA into the blank electrolyte. Combined with the self-discharge tests, XPS, and EDX results, the self-discharge and transition metal dissolution of $\text{LiNi}_{0.5}\text{Mn}_{1.5}\text{O}_4$ were suppressed effectively. As a result, the cycling

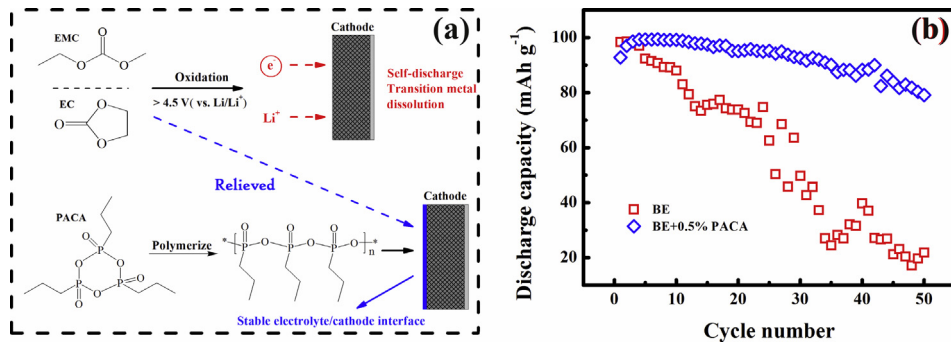


Fig. 9. Schematic diagram to illustrate the beneficial effect of PACA on $\text{LiNi}_{0.5}\text{Mn}_{1.5}\text{O}_4$ cathode material (a), the cycling performance of the $\text{Li}/\text{LiNi}_{0.5}\text{Mn}_{1.5}\text{O}_4$ cells in the electrolyte with and without PACA at elevated temperatures (b).

performance of $\text{LiNi}_{0.5}\text{Mn}_{1.5}\text{O}_4$ at elevated temperatures was enhanced significantly, although the capacity retention almost remained the same at room temperature.

Acknowledgments

The authors are grateful for the financial support from the National Basic Research Program of China (973 Program 2014CB643406), and the Major Special Plan of Science and Technology of Hunan Province, China (No. 2011FJ1005).

References

- [1] J.M. Tarascon, M. Armand, *Nature* 414 (2001) 359.
- [2] M. Hu, X. Pang, Z. Zhou, *J. Power Sources* 237 (2013) 229.
- [3] J. Wolfenstine, J. Allen, *J. Power Sources* 142 (2005) 389.
- [4] S. Okada, S. Sawa, M. Egashira, J.I. Yamaki, M. Tabuchi, H. Kageyama, T. Konishi, A. Yoshino, *J. Power Sources* 97–98 (2001) 430.
- [5] Q. Zhong, A. Bonakdarpour, M. Zhang, Y. Gao, J.R. Dahn, *J. Electrochem. Soc.* 144 (1997) 205.
- [6] H. Kawai, M. Nagata, H. Tukamoto, A.R. Westa, *Electrochem. Solid-State Lett.* 1 (1998) 212.
- [7] R. Santhanam, B. Rambabu, *J. Power Sources* 195 (2010) 5442.
- [8] L. Yang, B. Ravdel, B.L. Lucht, *Electrochem. Solid-State Lett.* 13 (2010) A95.
- [9] S.R. Li, N.N. Sinha, C.H. Chen, K. Xu, J.R. Dahn, *J. Electrochem. Soc.* 160 (2013) A2014.
- [10] N.P.W. Pieczonka, Z. Liu, P. Lu, K.L. Olson, J. Moote, B.R. Powell, J.H. Kim, *J. Phys. Chem. C* 117 (2013) 15947.
- [11] E.S. Lee, K.W. Nam, E. Hu, A. Manthiram, *Chem. Mater.* 24 (2012) 3610.
- [12] L. Hu, Z. Zhang, K. Amine, *J. Power Sources* 236 (2013) 175.
- [13] Z. Zhang, L. Hu, H. Wu, W. Weng, M. Koh, P.C. Redfern, L.A. Curtiss, K. Amine, *Energy Environ. Sci.* 6 (2013) 1806.
- [14] T. Kitagawa, K. Azuma, M. Koh, A. Yamauchi, M. Kagawa, H. Sakata, H. Miyawaki, A. Nakazono, H. Arima, M. Yamagata, M. Ishikawa, *Electrochemistry* 5 (2010) 345.
- [15] J. Xiang, F. Wu, R. Chen, L. Li, H. Yu, *J. Power Sources* 233 (2013) 115.
- [16] A. Lewandowski, A. Świderska-Mocek, *J. Power Sources* 194 (2009) 601.
- [17] A. Abouimrane, I. Belharouak, K. Amine, *Electrochim. Commun.* 11 (2009) 1073.
- [18] N. Shao, X.G. Sun, S. Dai, D.E. Jiang, *J. Phys. Chem. B* 116 (2012) 3235.
- [19] K. Xu, *J. Electrochem. Soc.* 145 (1998) L70.
- [20] Z. Wang, N. Dupré, L. Lajaunie, P. Moreau, J.F. Martin, L. Boutafa, S. Patoux, D. Guyomard, *J. Power Sources* 215 (2012) 170.
- [21] V. Tarnopolskiy, J. Kalhoff, M. Nádherná, D. Bresser, L. Picard, F. Fabre, M. Rey, S. Passerini, *J. Power Sources* 236 (2013) 39.
- [22] M. Xu, L. Zhou, Y. Dong, Y. Chen, A. Garsuch, B.L. Lucht, *J. Electrochem. Soc.* 160 (2013) A2005.
- [23] S. Dalavi, M. Xu, B. Knight, B.L. Lucht, *Electrochim. Solid-State Lett.* 15 (2012) A28.
- [24] A. von Cresce, K. Xu, *J. Electrochem. Soc.* 158 (2011) A337.
- [25] G. Yan, X. Li, Z. Wang, H. Guo, C. Wang, *J. Power Sources* 248 (2014) 1306.
- [26] K.C. Xu, A.V.W. Cresce, U.S. Patent 20,120,225,359, 2012.
- [27] A. Llanes García, *Synlett* 8 (2007) 1328.
- [28] X. Wen, J.E. Bakali, R. Deprez-Poulain, B. Deprez, *Tetrahedron Lett.* 53 (2012) 2440.
- [29] S. Ivanova, E. Zhecheva, R. Stoyanova, D. Nihtianova, S. Wegner, P. Tzvetkova, S. Simova, *J. Phys. Chem. C* 115 (2011) 25170.
- [30] D. Gryffroy, R.E. Vandenberghe, *J. Phys. Chem. Solids* 53 (1992) 777.
- [31] R. Alcántara, M. Jaraba, P. Lavela, J.L. Tirado, *Chem. Mater.* 16 (2004) 1573.
- [32] A.W. Moses, H.G.G. Flores, J.G. Kim, M.A. Langell, *Appl. Surf. Sci.* 253 (2007) 4782.
- [33] M. Caffio, B. Cortigiani, G. Rovida, A. Atrei, C. Giovanardi, *J. Phys. Chem. B* 108 (2004) 9919.
- [34] A.N. Mansour, *Surf. Sci. Spectra* 3 (1994) 279.
- [35] J.C. Carver, G.K. Schweitzer, T.A. Carlson, *J. Chem. Phys.* 57 (1972) 973.
- [36] R. Dedryvère, D. Foix, S. Franger, S. Patoux, L. Daniel, D. Gonbeau, *J. Phys. Chem. C* 114 (2010) 10999.
- [37] A. Manthiram, *J. Phys. Chem. Lett.* 2 (2011) 176.
- [38] S. Patoux, L. Daniel, C. Bourbon, H. Lignier, C. Pagano, F. Le Cras, S. Jouanneau, S. Martinet, *J. Power Sources* 189 (2009) 344.